Liquid freshwater accumulation in the Beaufort Gyre is constrained by sea ice-ocean stress feedback

Qiang Wang^{1,2}, John Marshall³, Jeffery Scott³, Gianluca Meneghello³, Sergey
Danilov^{1,4}, Thomas Jung^{1,5}

 1 Alfred Wegener Institute, Helmholtz Centre for Polar and Marine Research, Bremerhaven, Germany 2 Laboratory for Regional Oceanography and Numerical Modeling, Qingdao National Laboratory for

 ${\it Marine Science and Technology, Qingdao, China} {\it ^3} Department of Earth, Atmospheric and Planetary Sciences, Massachusetts Institute of Technology, and Massachu$

Cambridge, Massachusetts, USA

⁴Department of Mathematics and Logistics, Jacobs University, Bremen, Germany

⁵Institute of Environmental Physics, University of Bremen, Bremen, Germany

Key Points:

10 11

12

13

14

15

- Sea ice-ocean stress feedback causes an upwelling anomaly because ocean accelerates more than ice during wind-driven Beaufort Gyre spin-up
- The feedback significantly limits freshwater accumulation in the Beaufort Gyre
- Weaker sea ice accelerates more strongly in response to anticyclonic winds and geostrophic currents, leading to more freshwater accumulation

Corresponding author: Qiang Wang, Qiang.Wang@awi.de

Abstract

Based on satellite observations it has been hypothesized that the stress coupling between sea ice and ocean limits freshwater accumulation in the Beaufort Gyre (BG) through a negative feedback. For the first time this hypothesis is tested using global sea ice-ocean model simulations in this paper. The model results reveal the operation of the sea ice-ocean stress feedbacks regulating the gyre. We find that the stress feedback significantly limits liquid freshwater accumulation when an anticyclonic wind anomaly spins up the BG. The stress feedback becomes weaker when sea ice becomes weaker and accelerates more strongly in response to the spin-up of the anticyclonic geostrophic ocean currents under the wind forcing anomaly. Our study suggests that, with weaker sea ice in a warmer climate, the BG can store more freshwater due to stronger responses of sea ice to anticyclonic winds, and the accompanying weakening of the stress feedback can further increase the potential of freshwater accumulation.

1 Introduction

The Beaufort Gyre (BG) is the largest freshwater reservoir of the Arctic Ocean. Because of the potential impact of the Arctic freshwater on the large scale ocean circulation and climate [Aagaard et al., 1985], understanding the freshwater dynamics of the BG region has drawn much attention in the scientific community for decades [see the review by Proshutinsky et al., 2015].

Freshwater accumulation in the BG is driven by the anticyclonic wind associated with the high atmospheric pressure over the BG region. Hence, variations of BG liquid freshwater content (FWC) are correlated with the changes in the atmospheric circulation regimes [Proshutinsky et al., 2002, 2009]. The accumulation of freshwater by the wind-driven Ekman convergence and downwelling is counteracted by mesoscale eddy transport, and the balance of these two effects acts to maintain the level of freshwater storage in the gyre [Davis et al., 2014; Lique et al., 2015; Manucharyan and Spall, 2016; Yang et al., 2016]. Changes in freshwater sources and in freshwater circulation pathways modulated by wind forcing are also able to change the FWC in the Canadian Basin and BG [Krishfield et al., 2014; Morison et al., 2012; Yamamoto-Kawai et al., 2009].

The FWC in the BG has increased dramatically during the last two decades [Giles et al., 2012; Proshutinsky et al., 2015; Rabe et al., 2014; Zhang et al., 2016], with eddy activity enhanced [Zhao et al., 2016]. It has been suggested that the rapid Arctic sea ice decline contributed to about half of the freshwater accumulated in the BG by supplying both ice meltwater and freshwater of other origins to the BG [Wang et al., 2018]. Spatial redistribution of meteoric water towards the western Arctic can explain a large part of the FWC increase in the Canada Basin [Alkire et al., 2017].

Recent satellite observations of sea surface height (SSH) indicate that the anticyclonic geostrophic currents became stronger with the accumulation of freshwater in the BG [Armitage et al., 2016, 2017]. In the meantime faster sea ice drift is also observed [Spreen et al., 2011; Petty et al., 2016]. However, sea ice drift did not speed up as much as the ocean did, in particular in winter months [Dewey et al., 2018; Meneghello et al., 2018]. The sea ice-ocean stress is a function of the relative velocity between the sea ice and ocean. Based on observations and analysis of model output, a sea ice-ocean stress negative feedback for BG freshwater accumulation was conjectured: A strong increase in the anticyclonic ocean velocity and the smaller changes in sea ice velocity may together result in a reduction in the BG region downwelling (an upwelling anomaly) and possibly a net upwelling during winter, which may act to constrain freshwater accumulation [Dewey et al., 2018; Meneghello et al., 2018; Zhong et al., 2018]. This feedback is dubbed the 'ice-ocean governor' in an accompanying paper by Meneghello et al. (submitted).

In this study we explore the existence of the sea ice-ocean stress feedback and quantify its effect on freshwater accumulation in the BG by using numerical simulations. For the first time, the impact of the stress feedback on the BG FWC is explicitly derived from dedicated sensitivity experiments using a global model with realistic ocean and sea ice configurations.

2 Model Description

We use the Finite Element Sea Ice-Ocean Model [FESOM, Wang et al., 2014] in this work. FESOM is a multi-resolution ocean general circulation model based on an unstructured-mesh method [Danilov et al., 2004; Wang et al., 2008]. We apply a global setup with nominal 1° horizontal resolution in most parts of the ocean and 24 km north of 45°N. The resolution is also refined along the coast and in the equatorial band. In the vertical 47 z-levels are used with 10 m resolution in the upper 100 m depth. This mesh has been used in previous model intercomparison studies on the Arctic Ocean liquid and solid freshwater budget and content [Wang et al., 2016a,b].

The ocean is initialized with temperature and salinity from the Polar Science Center Hydrographic Climatology v.3 [Steele et al., 2001] and zero velocity, and sea ice is initialized with a field obtained from a previous simulation. A control simulation forced by the repeating normal year atmospheric data set [Large and Yeager, 2009] is carried out for 60 years. Branching out from the 30th year of the control run, one sensitivity simulation (named as BGplus) is made following the protocol of BG wind anomaly experiments described by Marshall et al. [2017]. A constant-in-time anticyclonic wind anomaly centered over the BG is added to the wind forcing (Fig. 1a), and the model is run for 30 years.

The daily mean SSH $(\eta_{control})$ is saved from the control run. We carried out another sensitivity simulation, which is the same as BGplus except that we replace the geostrophic velocity with that in the control run for the calculation of the stress between sea ice and ocean. That is, the ocean surface velocity used in the stress calculation during the model simulation is modified to $u_{oce}^{new} = u_{oce} - g/f\partial_y(\eta_{control} - \eta_{instant})$ and $v_{oce}^{new} = v_{oce} + g/f\partial_x(\eta_{control} - \eta_{instant})$, where $\eta_{instant}$ is the SSH simulated at the current model time step, g is the gravity acceleration and f the Coriolis parameter. By modifying the calculation of the stress we intentionally eliminate the feedback of the sea ice-ocean coupling through geostrophic currents. This simulation is called BGplus/noGeo hereafter. We repeated the control run with the stress calculation modified as described above and found that the model result is indistinguishable from the control run, which indicates that the daily output of SSH from the control run is enough for our purpose to investigate the effect of the stress feedback.

The simulations described above are referred to as the reference experiment. Another three experiments are conducted to assess robustness of the stress feedback to varying wind anomaly strength and two model parameters (called wind/2, GM3, and P/2, respectively), while examing the full model parameter space is beyond the scope of this paper. In experiment wind/2, we reduce the magnitude of the anticyclonic wind anomaly to half of that used in the reference experiment. This experiment allows to investigate the stress feedback in the case of smaller wind perturbation. The eddy GM diffusivity [Gent and McWilliams, 1990] is $500 \,\mathrm{m}^2/\mathrm{s}$ in the reference experiment. This is broadly in accord with the value inferred from observations presented in Meneghello et al. [2017]. The GM diffusivity is increased to $1500 \,\mathrm{m}^2/\mathrm{s}$ in experiment GM3. This experiment will demonstrate the response of the stress feedback to the strength of eddy activities. Experiment P/2 is intended to explore the sensitivity to the sea ice strength parameter P^* . We reduce P^* from $27500 \,\mathrm{N/m}^2$ (the value suggested by Hibler and Walsh [1982]) in the reference experiment to $13750 \,\mathrm{N/m}^2$ in experiment P/2. Sea ice strength is proportional to $P = P^*h\exp[-\mathrm{C}(1-\mathrm{a})]$, where h is sea

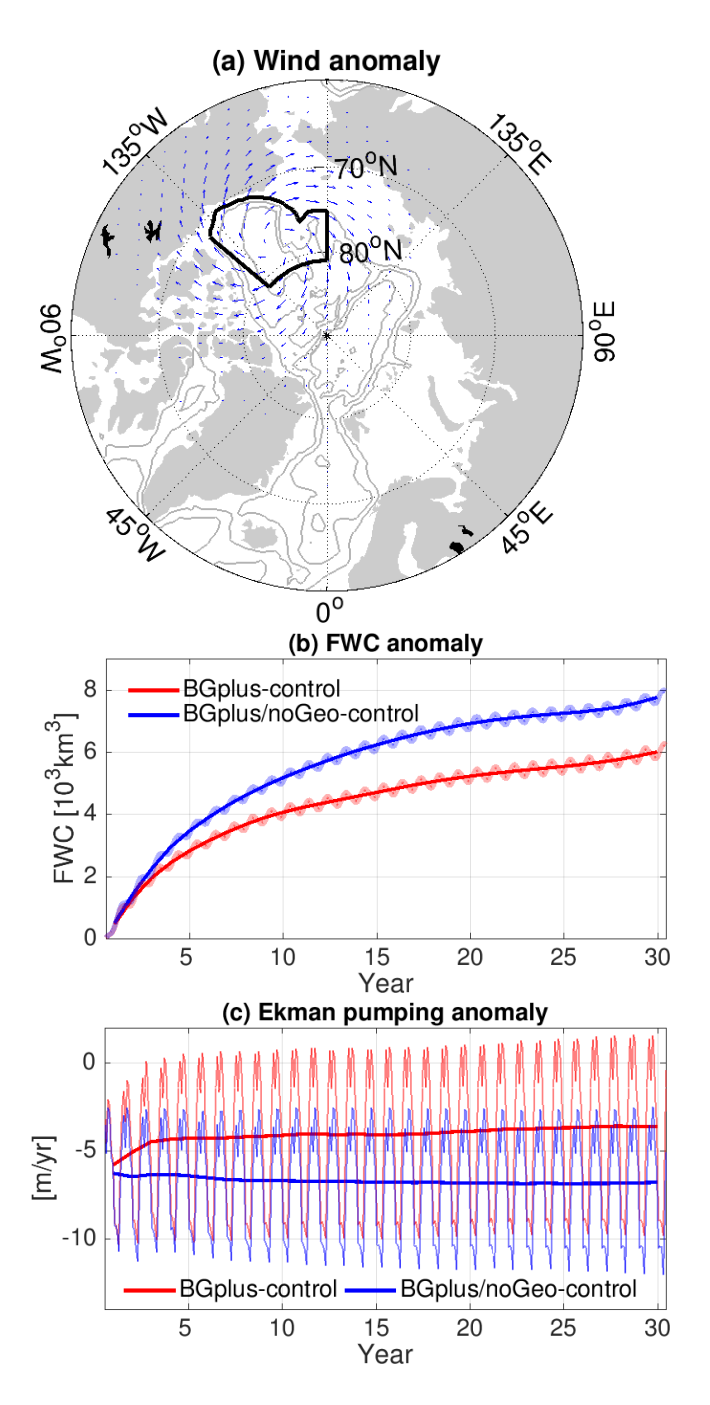


Figure 1. (a) The wind anomaly used in the sensitivity simulations of the reference experiment. The associated sea level pressure (SLP) anomaly is shown in the supporting information Fig. S1. The defined Beaufort Gyre (BG) region is indicated by the black box. (b) The anomaly of the BG liquid freshwater content (FWC) in BGplus and BGplus/noGeo referenced to the control run. (c) The anomaly of BG Ekman pumping referenced to the control run. Annual means are shown together with monthly means. The results are for the 'reference' experiments.

ice thickness, C=20, and a is sea ice concentration. Therefore, this experiment resembles a condition when sea ice is weaker. Although we change the sea ice strength by reducing P^* in this experiment, it can also provide implication on the response of the stress feedback to sea ice weakening (smaller P) induced by reduction in sea ice concentration or thickness in a warmer climate.

In each experiment we carry out a 60 year control run, a 30 year BGplus run and a 30 year BGplus/noGeo run. In total 11 simulations are conducted and analyzed (the control run of reference and wind/2 is the same).

3 Results

3.1 Reference experiment

In the control run of the reference experiment, the liquid FWC (calculated using a reference salinity of 34.8 and integrated from surface to the depth of the reference salinity) in the BG is in an equilibrium state during the last 30 years (Fig. S2a). The seasonal oscillation in the FWC is due to the seasonal variation of both freshwater availability and Ekman pumping. After adding the anticyclonic wind anomaly, the FWC increases with time in the BGplus simulation (Fig. S2a and Fig. 1b). The inflation rate of the FWC starts to saturate with time, as expected from the counteracting effects of eddies. When the sea ice-ocean stress feedback is eliminated (the simulation BGplus/noGeo), the increase of the FWC induced by the imposed wind anomaly is larger. The negative stress feedback reduces the accumulation of freshwater by about 25% at the end of the simulations (Fig. 1b).

The accumulation of liquid freshwater in the BG under the anticyclonic wind anomaly is consistent with the enhanced Ekman downwelling (Fig. S2b and Fig. 1c). The stress feedback reduces the Ekman downwelling, and thus the freshwater accumulation (Fig. 1b,c). The most pronounced changes in the Ekman pumping take place during the first 2-3 years of the simulation BGplus (Fig. 1c). To better illustrate the seasonal variability and temporal evolution of the Ekman pumping, we show the monthly mean difference between the sensitivity runs and the control run over three different periods in Fig. 2a-c. In the first year, the impact of the anticyclonic wind anomaly on Ekman pumping is very similar in the two sensitivity runs: The Ekman downwelling is enhanced in all the seasons, although the impact is much smaller in winter when the BG is almost fully covered by sea ice (Fig. 2a and Fig. 2g). The Ekman downwelling changes only marginally with time in simulation BGplus/noGeo, while a significant reduction in the Ekman downwelling takes place from November to the following June in simulation BGplus (Fig. 2b,c). In fact, during some winter months, the anticyclonic wind anomaly even leads to a positive Ekman pumping anomaly (that is, reducing the Ekman downwelling) after a few years into the simulation BGplus (Fig. 1c and Fig. 2b,c). As a consequence of this seasonality, the difference of the Ekman pumping between the two sensitivity runs shows a clear annual cycle (Fig. 2d).

The stress between the sea ice and ocean is determined by their relative velocity. The differences between the two sensitivity runs in sea ice speed (Fig. 2e) and ocean surface speed (the one used in the calculation of the stress, Fig. 2f) reveal that the seasonal variation of the Ekman pumping difference is mainly due to sea ice speed differences. Indeed, when the sea ice-ocean stress feedback is eliminated in BGplus/noGeo, both the sea ice speed and ocean surface speed (the one used in the calculation of the stress) do not show significant changes during the 30 years simulation (Fig. S3,4). On the contrary, in simulation BGplus, the ocean surface speed increases in all the seasons following the increase of the liquid FWC and SSH with time, while the sea ice speed increases much less significantly in months when sea ice concentration is high (close to be 100%). The latter is because the sea ice internal

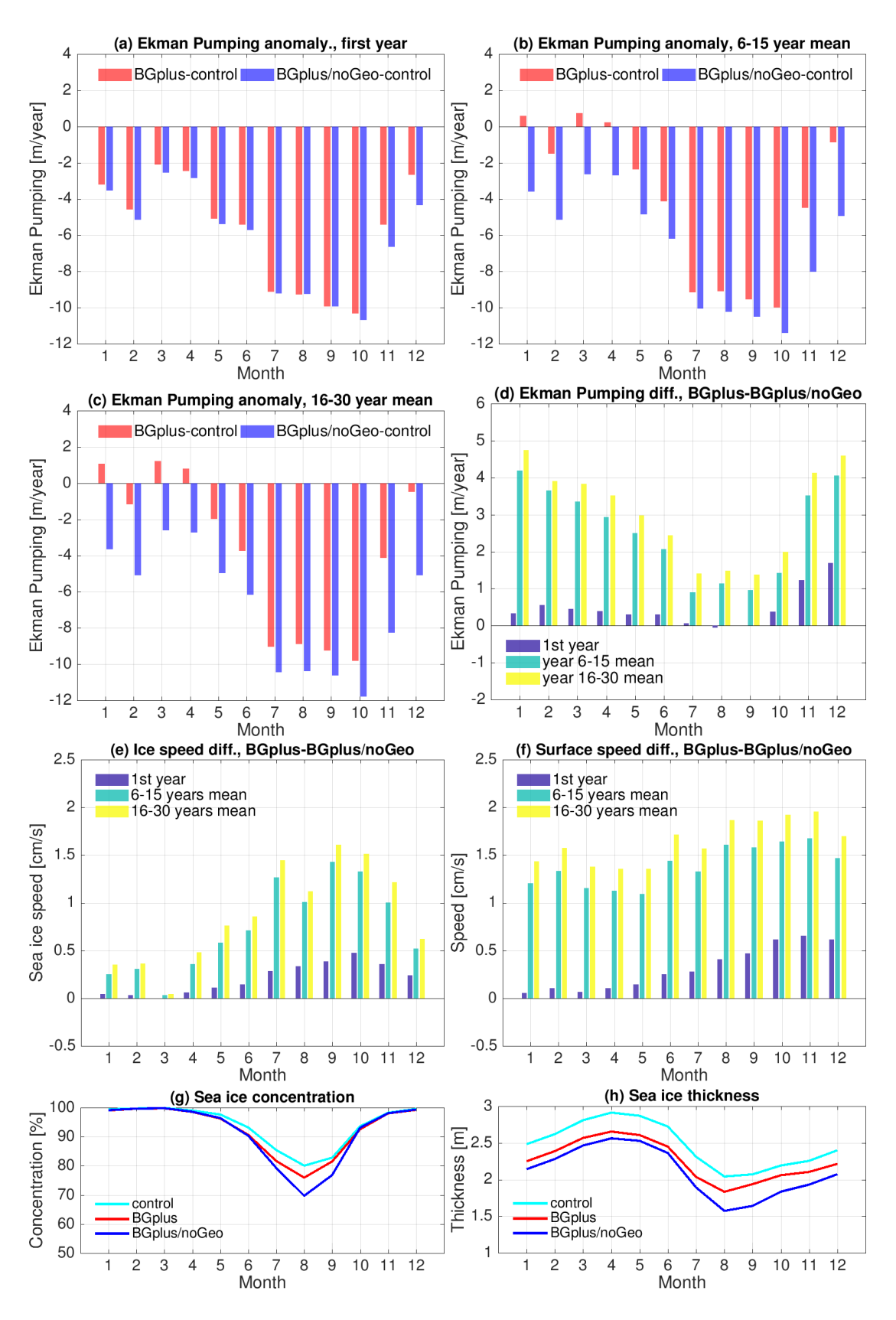


Figure 2. The anomaly of the Ekman pumping averaged over the Beaufort Gyre (BG) refereced to the control run: (a) in the first year, (b) averaged from year 6 to year 15, (c) averaged from year 16 to 30. (d) The difference of the BG Ekman pumping between BGplus/noGeo and BGplus. (e) The difference of the BG sea ice speed between BGplus/noGeo and BGplus. (f) The same as (e) but for the ocean surface speed. In (f) the ocean speed is the one used in the calculation of ice-ocean stress. (g) Mean BG sea ice concentration averaged from year 16 to 30. (h) The same as (g) but for sea ice thickness. The results are for the 'reference' experiment.

stress, which strongly depends on the sea ice concentration, is the predominant factor controlling the sea ice momentum balance in this case. Therefore, our results suggest that the sea ice-ocean stress feedback is more effective when sea ice concentration is very high (cf. Fig. 2d and Fig. 2g).

Although the wind anomaly and eliminating the stress feedback tend to reduce the mean sea ice concentration in the BG only in summer months (Fig. 2g), they reduce the sea ice thickness in all the seasons dynamically, including winter (Fig. 2h). Thinner sea ice implies smaller internal stress and higher mobility. The sea ice thickness in the BG evolves with time (Fig. S5), but changes in sea ice speed between different periods in the BGplus/noGeo simulation are very small in the months when sea ice concentration is high and the stress feedback plays an important role (Fig. S3). This means that the imbedded second feedback loop through changing sea ice thickness does not play a vital role in our simulations.

3.2 Sensitivity experiments

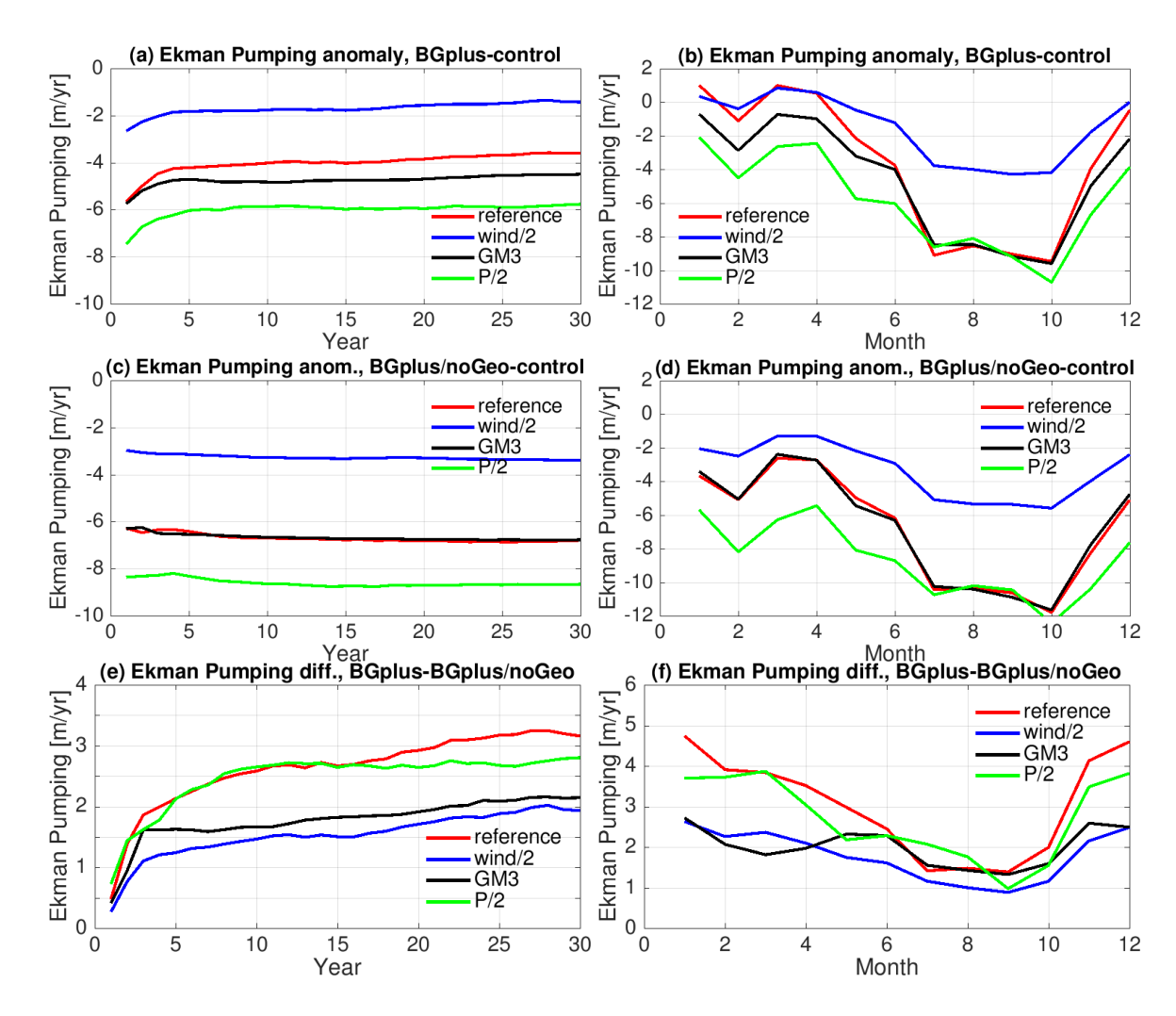


Figure 3. The difference of the Ekman pumping over the Beaufort Gyre (BG) between BG-plus and the control run: (a) the time series of the annual mean and (b) the seasonal cycle averaged from year 16 to 30. (c)(d) The same as (a)(b) but for the difference between BG-plus/no-Geo and control. (e)(f) The same as (a)(b) but for the difference between BG-plus and BG-plus/no-Geo.

Similar to the reference experiment, the imposed anticyclonic wind anomaly enhances Ekman downwelling in the BGplus setups of all other sensitivity experiments (Fig. 3a). Moreover, all the sensitivity experiments show that the Ekman downwelling weakens during the first few years, when the liquid FWC increases rapidly (cf. Fig. 3a and Fig. 4a). In simulations with the sea ice-ocean stress feedback eliminated (BGplus/noGeo), the Ekman downwelling does not show rapid initial weakening (Fig. 3c), and it is stronger than in their BGplus counterparts (Fig. 3e). The wind anomaly enhances the Ekman downwelling the most significantly in summer (Fig. 3b,d), while the effect of the sea ice-ocean stress feedback on the Ekman pumping is the strongest in winter (Fig. 3f).

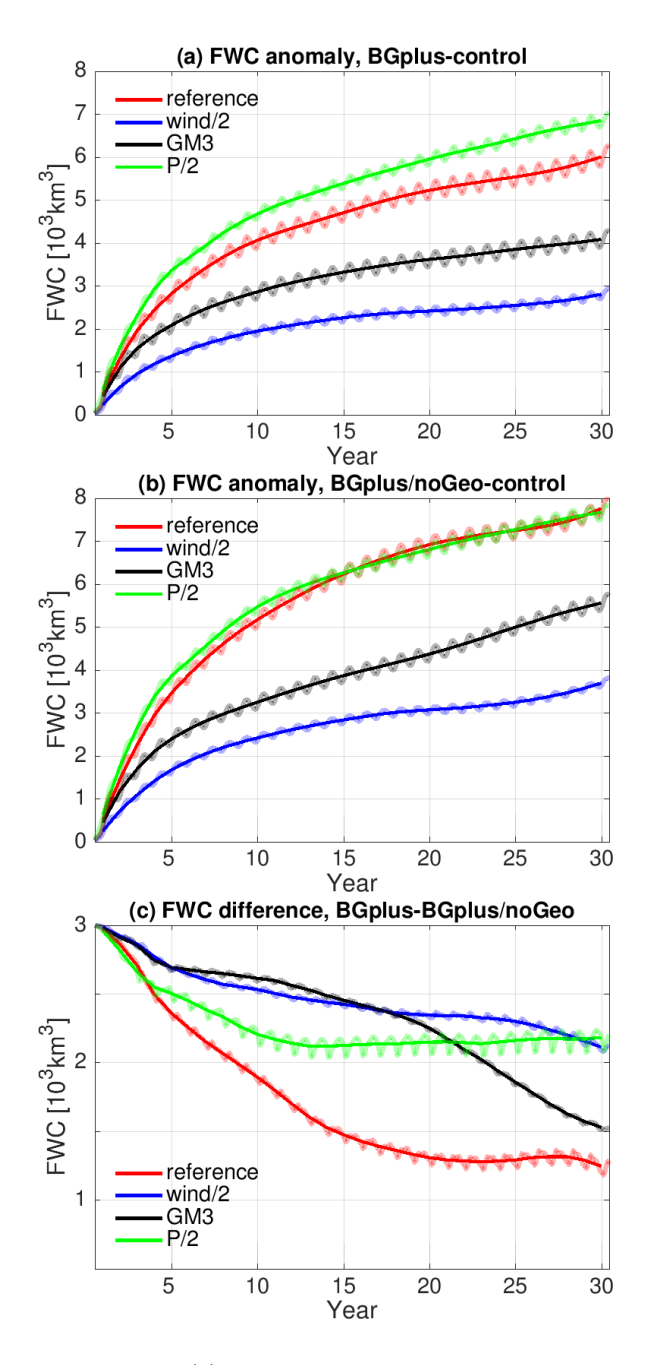
When the magnitude of the wind anomaly is reduced (experiment wind/2), the strength of the Ekman downwelling anomaly is reduced in all the months (Fig. 3d). However, when the stress feedback is included, the Ekman downwelling anomalies in the winter months do not change much between the two experiments (Fig. 3b). This is because a stronger wind anomaly in the reference experiment leads to more freshwater accumulation (Fig. 4a), and thus a stronger impact on the Ekman pumping from the stress feedback (Fig. 3f).

Furthermore, the Ekman pumping anomaly induced by the wind anomaly does not change when the eddy diffusivity is changed, provided that the sea ice-ocean stress feedback is eliminated (experiment GM3, Fig. 3c,d). In contrast, with the stress feedback active, the Ekman downwelling is stronger with a higher eddy diffusivity in the months when the BG is nearly fully covered by sea ice (Fig. 3b). This is because a higher eddy diffusivity leads to a lower FWC in the BG (Fig. 4a), and thus a weaker constraint on the Ekman downwelling from the stress feedback in the months when it plays a role (Fig. 3f).

The experiment P/2 represents a case of weaker sea ice. With the same anticyclonic wind anomaly, weaker sea ice leads to stronger Ekman downwelling in the months when sea ice concentration is close to 100% (Fig. 3b). This results in stronger freshwater accumulation (Fig. 4a). However, the effect of the sea ice-ocean stress feedback on Ekman pumping is weaker than in the reference experiment (Fig. 3e,f). With weaker sea ice, the ocean geostrophic velocity enhances the sea ice velocity more significantly, especially in cold seasons (Fig. S6), leading to a smaller change in the relative velocity between the sea ice and ocean, thus a weaker impact of the stress feedback on Ekman pumping.

As a consequence of modifying the Ekman pumping, the stress feedback acts to limit the freshwater accumulation in the BG in all the experiments (Fig. 4c). However, the impacts on the BG liquid FWC are not just determined by the changes in Ekman pumping (cf. Fig. 4c and Fig. 3f). For example, at the end of the simulations, the FWC anomaly induced by the stress feedback is the smallest in experiment P/2, although the induced anomaly in the Ekman pumping is not. This can be partly explained by the fact that the total BG FWC is the highest in this experiment (Fig. S7), which implies steeper isopycnal slope and thus a stronger counteracting effect of eddies.

The anticyclonic wind anomaly increases the Ekman downwelling and freshwater accumulation in the BG (Fig. S8a and Fig. S9a). The stress feedback reduces the Ekman downwelling in the western BG and tends to enhance it along the southern and eastern coast of the Beaufort Sea (Fig. S8b,c). Note that the Ekman transport anomaly induced by eliminating the stress feedback is also directed towards the western BG (Fig. S10a,b). Consequently the FWC anomaly induced by the stress feedback is centered at the western boundary of the BG (Fig. S9c). Under the anticyclonic wind anomaly, the center of the gyre circulation moves towards the northwest along with the increase of FWC (Fig. S11), which is consistent with the observed movement of the BG



211

212

213

Figure 4. (a) The difference of the liquid freshwater content (FWC) in the Beaufort Gyre (BG) region between BGplus and control. (b) The same as (a) but for the difference between BGplus/noGeo and control. (c) The same as (a) but for the difference between BGplus and BGplus/noGeo.

centroid location accompanying the BG FWC increase in recent years [Armitage et al., 2017]. Our simulations indicate that the stress feedback tends to retard the change of the centroid location. A similar finding about the impact of the stress feedback on freshwater spatial distribution is evident from the other experiments (Fig. S8,9,10).

4 Discussions and conclusions

This study explicitly illustrated the sea ice-ocean stress feedback and quantified its effect by using global model simulations. When an anticyclonic wind forcing is enforced over the Beaufort Gyre (BG) in our simulations, freshwater is accumulated, leading to increases in sea surface height (SSH) and thus in anticyclonic geostrophic velocity in the gyre. At the same time sea ice also accelerates. However, due to the large internal stress of sea ice in months when its concentration is close to 100%, its speed-up is relatively small. This results in an Ekman upwelling anomaly in the BG, which significantly limits freshwater accumulation. Our study supports the notion of the existence of sea ice-ocean stress feedback, which has been postulated based on observations [Dewey et al., 2018; Meneghello et al., 2018; Zhong et al., 2018].

Even without the sea ice-ocean stress feedback, sea ice blocks the momentum transfer from the atmosphere to the ocean in months when its internal stress is high. Compared to the summer sea ice situation, winter sea ice weakens the response of the Ekman pumping to the applied wind anomaly by about 8 m/yr (in our reference experiment). With the stress feedback included, the winter response decreases by about a further 4 m/yr, thus resulting in nearly zero Ekman pumping response to the wind forcing during some winter months. This indicates that the stress feedback accounts for approximately one third of the total blocking effect of sea ice in its winter condition relative to its summer condition. Further experiments reveal that the ratio depends on the experimental setups. For example, in the experiment with a reduced ice strength parameter, although the change in Ekman pumping induced by the stress feedback is weaker than in the reference experiment, it now accounts for about half of the total blocking effect in winter. This is because the total blocking effect is smaller with weaker sea ice.

By reducing Ekman downwelling the stress feedback significantly limits freshwater accumulation. This effect is found in all the model setups used in this study, while the quantitative impact on the freshwater content (FWC) depends on the details of the model configurations. For example, the accumulation of freshwater depends also on the counteracting eddy transport, and thus the slope of isopycnals, that is, the FWC state itself. In the experiment with lower sea ice strength, the total FWC in the BG is higher. Therefore, the FWC anomaly induced by eliminating the stress feedback in this experiment is much smaller than in the reference experiment although the Ekman downwelling anomaly is only slightly smaller. The simulations also indicate that the stress feedback slows down the change of the BG centroid location.

Weaker sea ice with smaller internal stress allows for an overall stronger response of the Ekman pumping to the wind forcing anomaly. First, sea ice speeds up more significantly in response to stronger anticyclonic winds. Second, the strength of the stress feedback becomes weaker (that is, weaker sea ice speeds up more significantly in response to enhanced ocean surface geostrophic currents). The two factors together help to strengthen the response of Ekman downwelling to an anticyclonic wind regime, implying that the BG has the potential to accumulate more freshwater in a warmer climate. When the Arctic atmospheric wind regime changes in time, weaker sea ice will result in larger magnitudes in the variation of BG FWC. The variation could be further amplified by increasing availability of freshwater to the BG associated with, for example, sea ice decline [Wang et al., 2018] or enhanced river runoff and precipitation [Zhang et al., 2013; Haine et al., 2015; Carmack et al., 2016].

Although the sea ice-ocean stress feedback significantly limits the accumulation of freshwater in the BG in our simulations, it does not considerably reduce the time scale for the gyre to reach an equilibrium state when an anticyclonic wind forcing anomaly is imposed. In none of our simulations does the BG FWC reach an equilibrium state after the wind forcing anomaly has been imposed for 30 years. Changing the strength of the wind forcing anomaly and eddy diffusivity shows stronger impacts on the time scale of the gyre spin-up than the stress feedback. By using a coarse resolution model and parameterizing mesoscale eddies in this paper we are able to study the stress feedback under realistic ocean and sea ice conditions with affordable computing resources. However, the time scale of the gyre spin-up depends on the realism of the eddy diffusivity [Manucharyan and Spall, 2016]. Therefore, future work is required to better quantify the impact of the stress feedback on the gyre spin-up time scale by using eddy resolving Arctic Ocean models, which is still challenging.

Acknowledgments

The AWI group was supported by the Helmholtz Climate Initiative REKLIM (Regional Climate Change) of Germany. The MIT group was supported by the NSF Arctic Program and by NASA through the MIT-GISS collaborative agreement. The simulations were performed at the North-German Supercomputing Alliance (HLRN).

References

- Aagaard, K., J. H. Swift, and E. Carmack (1985), Thermohaline circulation in the Arctic mediterranean seas, *Journal of Geophysical Research-oceans*, 90, 4833–4846.
 - Alkire, M. B., J. Morison, A. Schweiger, J. Zhang, M. Steele, C. Peralta-Ferriz, and S. Dickinson (2017), A meteoric water budget for the Arctic Ocean, *J. Geophys. Res. Oceans*, 122, 10,020–10,041.
 - Armitage, T., S. Bacon, A. Ridout, S. Thomas, Y. Aksenov, and D. Wingham (2016), Arctic sea surface height variability and change from satellite radar altimetry and GRACE, 2003-2014, *J. Geophys. Res. Oceans*, 121, 4303–4322.
 - Armitage, T., S. Bacon, A. Ridout, A. Petty, S. Wolbach, and M. Tsamados (2017), Arctic Ocean surface geostrophic circulation 2003–2014, *The Cryosphere*, 11, 1767–1780.
 - Carmack, E. C., M. Yamamoto-Kawai, T. W. N. Haine, S. Bacon, B. A. Bluhm, C. Lique, H. Melling, I. V. Polyakov, F. Straneo, M.-L. Timmermans, and W. J. Williams (2016), Freshwater and its role in the Arctic Marine System: Sources, disposition, storage, export, and physical and biogeochemical consequences in the Arctic and global oceans, J. Geophys. Res. Biogeosci., 121, 675–717.
 - Danilov, S., G. Kivman, and J. Schröter (2004), A finite-element ocean model: principles and evaluation, *Ocean Modell.*, 6, 125–150.
 - Davis, P. E. D., C. Lique, and H. L. Johnson (2014), On the link between Arctic sea ice decline and the freshwater content of the Beaufort Gyre: Insights from a simple process model, *Journal of Climate*, 27, 8170–8184.
- Dewey, S., J. Morison, R. Kwok, S. Dickinson, D. Morison, and R. Andersen (2018), Arctic iceocean coupling and gyre equilibration observed with remote sensing, *Geo-phys. Res. Lett.*, 45, 1499–1508.
- Gent, P. R., and J. C. McWilliams (1990), Isopycnal mixing in ocean circulation models, *J. Phys. Oceanogr.*, 20, 150–155.
- Giles, K. A., S. W. Laxon, A. L. Ridout, D. J. Wingham, and S. Bacon (2012), Western Arctic Ocean freshwater storage increased by wind-driven spin-up of the Beaufort Gyre, *Nature Geoscience*, 5, 194–197.
- Haine, T., B. Curry, R. Gerdes, E. Hansen, M. Karcher, C. Lee, B. Rudels, G. Spreen,
 L. de Steur, K. Stewart, and R. Woodgate (2015), Arctic freshwater export: Status,

mechanisms, and prospects, Global and Planetary Change, 125, 13–35.

- Hibler, W., and J. Walsh (1982), On modeling seasonal and interannual fluctuations of Arctic sea ice, *J. Phys. Oceanogr.*, 12, 1514–1523.
- Krishfield, R. A., A. Proshutinsky, K. Tateyama, W. J. Williams, E. C. Carmack, M. F. A., and M. L. Timmermans (2014), Deterioration of perennial sea ice in the Beaufort Gyre from 2003 to 2012 and its impact on the oceanic freshwater cycle, J. Geophys. Res. Oceans, 119, 1271–1305.
 - Large, W. G., and S. G. Yeager (2009), The global climatology of an interannually varying air-sea flux data set, *Climate Dynamics*, 33, 341–364.
 - Lique, C., H. L. Johnson, and P. E. D. Davis (2015), On the interplay between the circulation in the surface and the intermediate layers of the Arctic Ocean, *Journal of Physical Oceanography*, 45, 1393–1409.
 - Manucharyan, G., and M. Spall (2016), Winddriven freshwater buildup and release in the Beaufort Gyre constrained by mesoscale eddies, *Geophys. Res. Lett.*, 43, 273–282
 - Marshall, J., J. Scott, and A. Proshutinsky (2017), "climate response functions" for the Arctic Ocean: a proposed coordinated modelling experiment, Geoscientific Model Development, 10, 2833–2848.
 - Meneghello, G., J. Marshall, S. Cole, and M. L. Timmermans (2017), Observational inferences of lateral eddy diffusivity in the halocline of the Beaufort Gyre, *Geophys. Res. Lett.*, 44, 12,331–12,338.
 - Meneghello, G., J. Marshall, M. Timmermans, and J. Scott (2018), Observations of seasonal upwelling and downwelling in the Beaufort Sea mediated by sea ice, *J. Phys. Oceanogr.*, 48, 795–805.
 - Morison, J., R. Kwok, C. Peralta-Ferriz, M. Alkire, I. Rigor, R. Andersen, and M. Steele (2012), Changing Arctic Ocean freshwater pathways, *Nature*, 481, 66–70.
 - Petty, A., J. Hutchings, J. RichterMenge, and M. Tschudi (2016), Sea ice circulation around the Beaufort Gyre: The changing role of wind forcing and the sea ice state, J. Geophys. Res. Oceans, 121, 3278–3296.
 - Proshutinsky, A., R. H. Bourke, and F. A. McLaughlin (2002), The role of the Beaufort Gyre in Arctic climate variability: Seasonal to decadal climate scales, *Geophysical Research Letters*, 29, 2100.
 - Proshutinsky, A., R. Krishfield, M.-L. Timmermans, J. Toole, E. Carmack, F. McLaughlin, W. J. Williams, S. Zimmermann, M. Itoh, and K. Shimada (2009), Beaufort Gyre freshwater reservoir: State and variability from observations, *Journal of Geophysical Research-oceans*, 114, C00A10.
 - Proshutinsky, A., D. Dukhovskoy, M. Timmermans, R. Krishfield, and J. Bamber (2015), Arctic circulation regimes, *Phil. Trans. R. Soc. A*, 373, 20140,160.
 - Rabe, B., M. Karcher, F. Kauker, U. Schauer, J. M. Toole, R. A. Krishfield, S. Pisarev, T. Kikuchi, and J. Su (2014), Arctic ocean basin liquid freshwater storage trend 1992-2012, *Geophysical Research Letters*, 41, 961–968.
- Spreen, G., R. Kwok, and D. Menemenlis (2011), Trends in Arctic sea ice drift and role
 of wind forcing: 1992–2009, Geophys. Res. Lett., 38 (doi:10.1029/2011GL048970),
 L19,501.
- Steele, M., R. Morley, and W. Ermold (2001), Phc: A global ocean hydrography with a high quality Arctic Ocean, *J. Climate*, 14, 2079–2087.
- Wang, Q., S. Danilov, and J. Schröter (2008), Finite element ocean circulation model based on triangular prismatic elements, with application in studying the effect of vertical discretization, J. Geophys. Res. Oceans, 113, C05,015.
- Wang, Q., S. Danilov, D. Sidorenko, R. Timmermann, C. Wekerle, X. Wang, T. Jung, and J. Schröter (2014), The Finite Element Sea Ice-Ocean Model (FESOM) v.1.4: formulation of an ocean general circulation model, *Geosci. Model Dev.*, 7, 663–693.

Wang, Q., M. Ilicak, R. Gerdes, H. Drange, Y. Aksenov, D. Bailey, M. Bentsen,
A. Biastoch, A. Bozec, C. Böning, C. Cassou, E. Chassignet, A. Coward, B. Curry,
G. Danabasoglu, S. Danilov, E. Fernandez, P. Fogli, Y. Fujii, S. Griffies, D. Iovino,
A. Jahn, T. Jung, W. Large, C. Lee, C. Lique, J. Lu, S. Masina, A. Nurser, B. Rabe,
C. Roth, D. Salas y Mélia, B. Samuels, P. Spence, H. Tsujino, S. Valcke, A. Voldoire,
X. Wang, and S. Yeager (2016a), An assessment of the Arctic Ocean in a suite
of interannual CORE-II simulations. Part I: Sea ice and solid freshwater, Ocean
Modell., 99, 110–132.

419

421

422

423

424

425

426

428

429

430

431

432

434

435

436

437

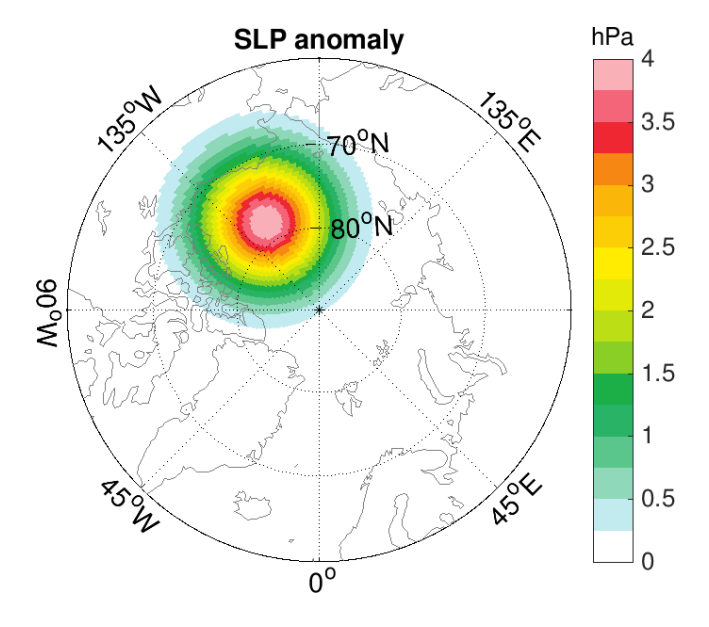
439

- Wang, Q., M. Ilicak, R. Gerdes, H. Drange, Y. Aksenov, D. Bailey, M. Bentsen,
 A. Biastoch, A. Bozec, C. Böning, C. Cassou, E. Chassignet, A. Coward, B. Curry,
 G. Danabasoglu, S. Danilov, E. Fernandez, P. Fogli, Y. Fujii, S. Griffies, D. Iovino,
 A. Jahn, T. Jung, W. Large, C. Lee, C. Lique, J. Lu, S. Masina, A. Nurser, B. Rabe,
 C. Roth, D. Salas y Mélia, B. Samuels, P. Spence, H. Tsujino, S. Valcke, A. Voldoire,
 X. Wang, and S. Yeager (2016b), An assessment of the Arctic Ocean in a suite of
 interannual CORE-II simulations. Part II: Liquid freshwater, Ocean Modell., 99,
 65–90.
 - Wang, Q., C. Wekerle, S. Danilov, N. Koldunov, D. Sidorenko, D. Sein, B. Rabe, and T. Jung (2018), Arctic sea ice decline significantly contributed to the unprecedented liquid freshwater accumulation in the Beaufort Gyre of the Arctic Ocean, *Geophys. Res. Lett.*, 45.
 - Yamamoto-Kawai, M., F. A. McLaughlin, E. C. Carmack, S. Nishino, K. Shimada, and N. Kurita (2009), Surface freshening of the Canada Basin, 2003–2007: River runoff versus sea ice meltwater, *Journal of Geophysical Research: Oceans*, 114, C00A05.
- Yang, J., A. Proshutinsky, and X. Lin (2016), Dynamics of an idealized Beaufort Gyre: 1. the effect of a small beta and lack of western boundaries, J. Geophys. Res. Oceans, 121, 1249–1261.
- Zhang, J., M. Steele, K. Runciman, S. Dewey, J. Morison, C. Lee, L. Rainville, S. Cole, R. Krishfield, M.-L. Timmermans, and J. Toole (2016), The Beaufort Gyre intensification and stabilization: A model-observation synthesis, *Journal of Geophysical Research: Oceans*, 121(11), 7933–7952.
- Zhang, X., J. He, J. Zhang, I. Polyakov, R. Gerdes, J. Inoue, and P. Wu (2013), Enhanced poleward moisture transport and amplified northern high-latitude wetting trend, *Nature Climate Change*, 3, 47–51.
- Zhao, M., M.-L. Timmermans, S. Cole, R. Krishfield, and J. Toole (2016), Evolution of the eddy fields in the Arctic Ocean's Canada Basin, 2005-2015, Geophys. Res. Lett., 43, 8106-8114.
- Zhong, W., M. Steele, J. Zhang, and J. Zhao (2018), Greater role of geostrophic currents in ekman dynamics in the western Arctic Ocean as a mechanism for Beaufort Gyre stabilization, *J. Geophys. Res. Oceans*, 123, 149–165.

Supporting Information for

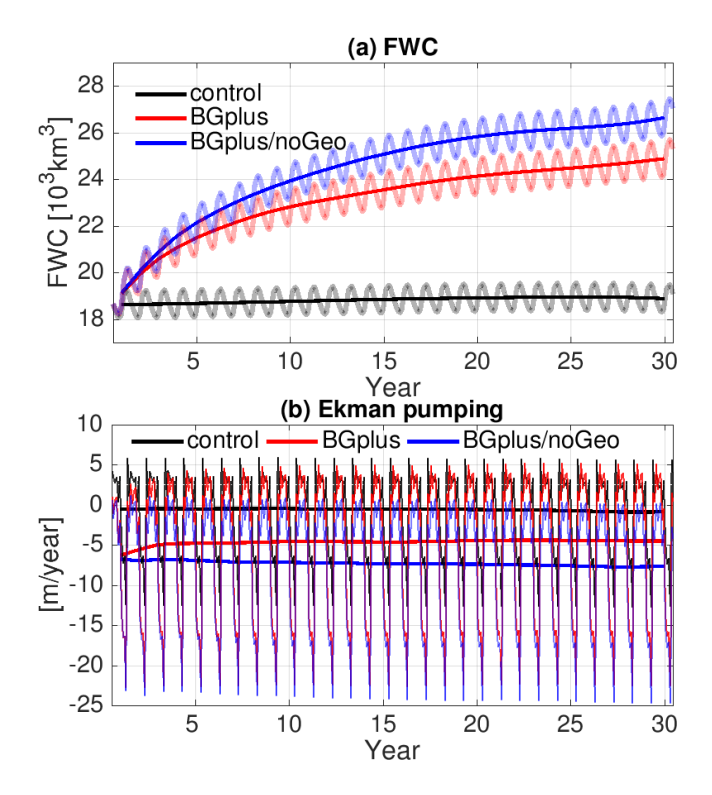
"Liquid freshwater accumulation in the Beaufort Gyre is constrained by sea ice-ocean stress feedback"

Qiang Wang*, John Marshall, Jeffery Scott, Gianluca Meneghello, Sergey Danilov, Thomas Jung

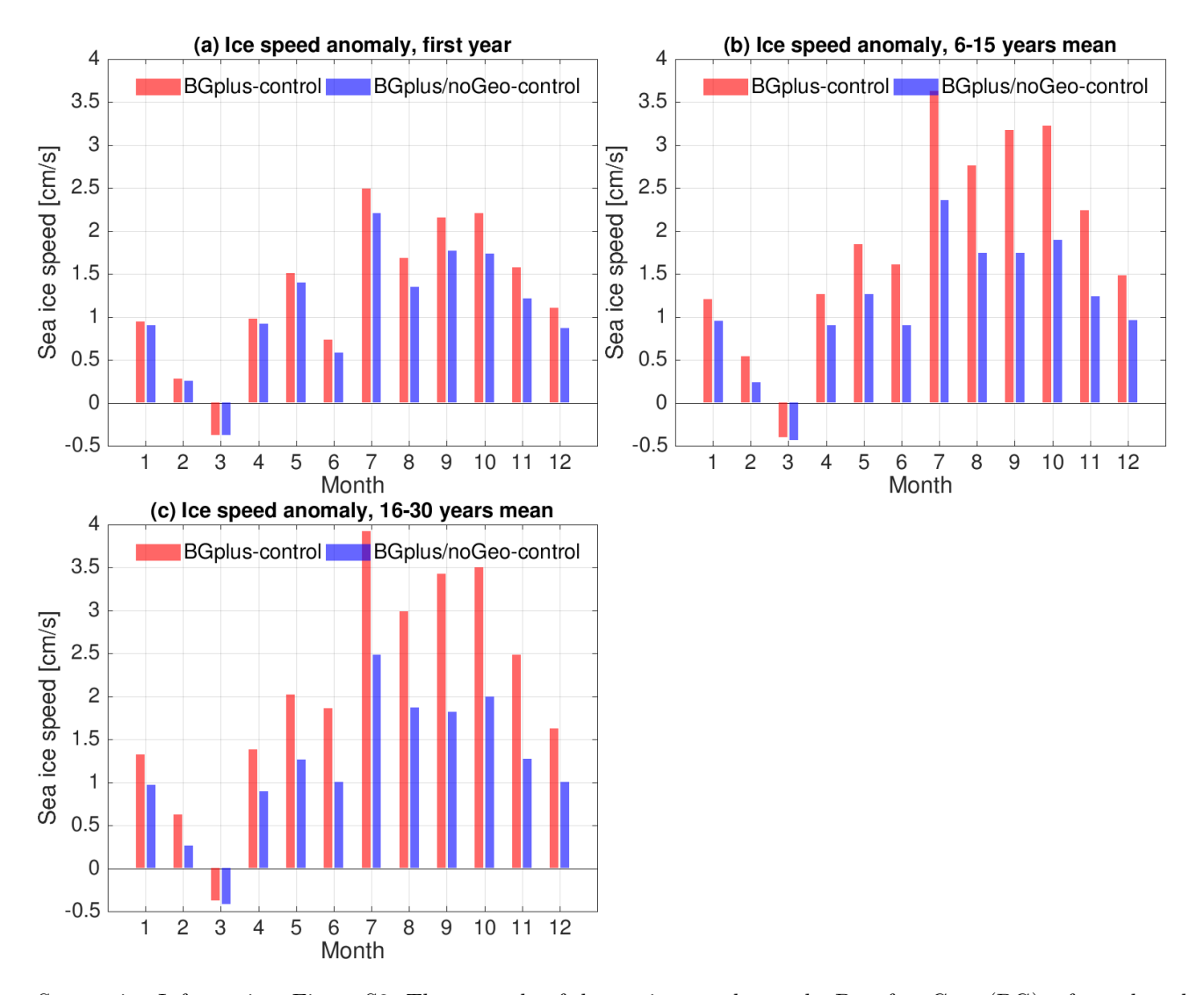


Supporting Information, Figure S1: The sea level pressure (SLP) anomaly used to derive the wind forcing anomaly (shown in Fig. 1a). The SLP anomaly has a maximum value of 4 hPa at the center. The anomaly fields are taken from Marshall et al. (2017).

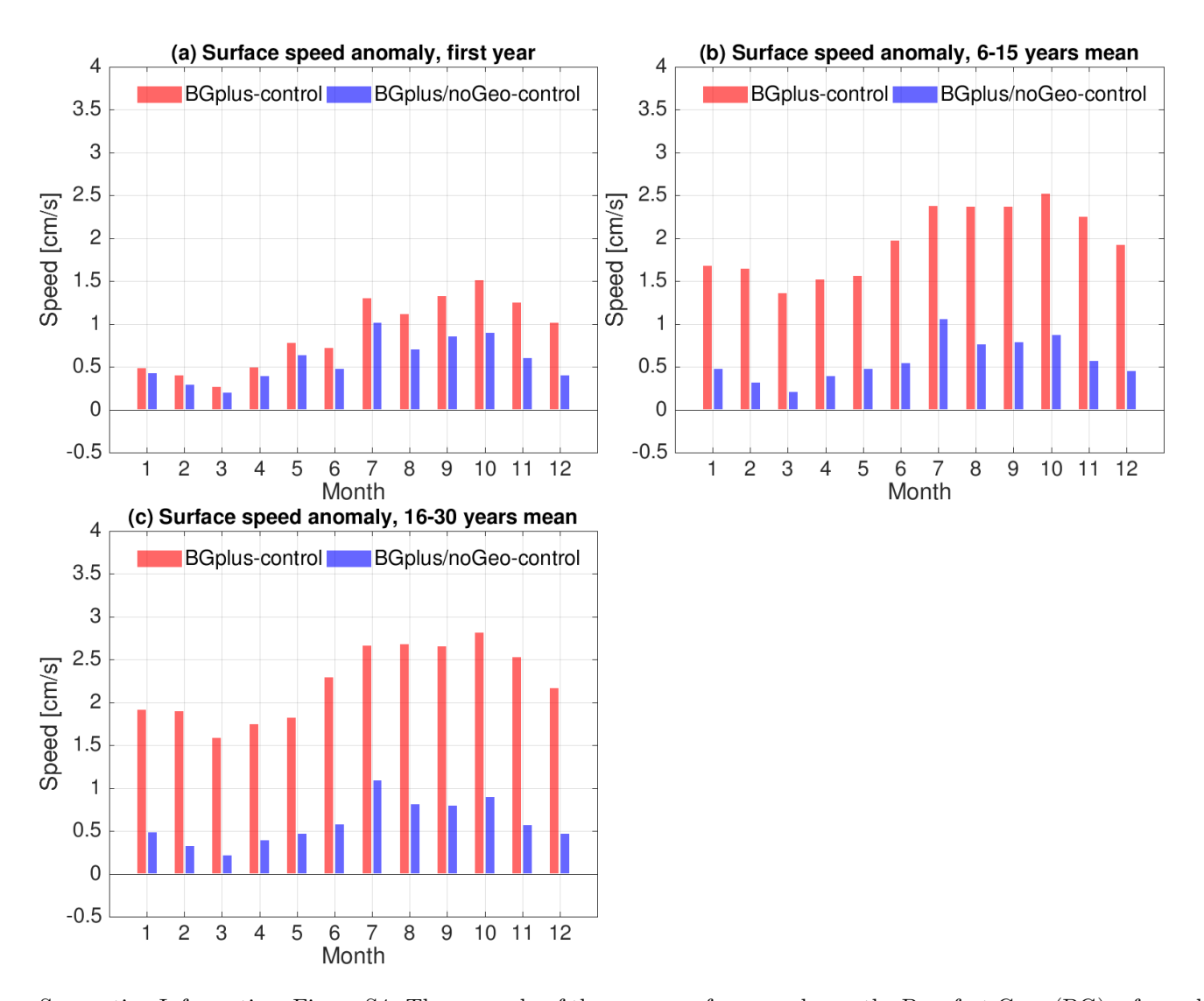
 $^{^*}$ Corresponding author: Qiang Wang, Qiang.Wang@awi.de



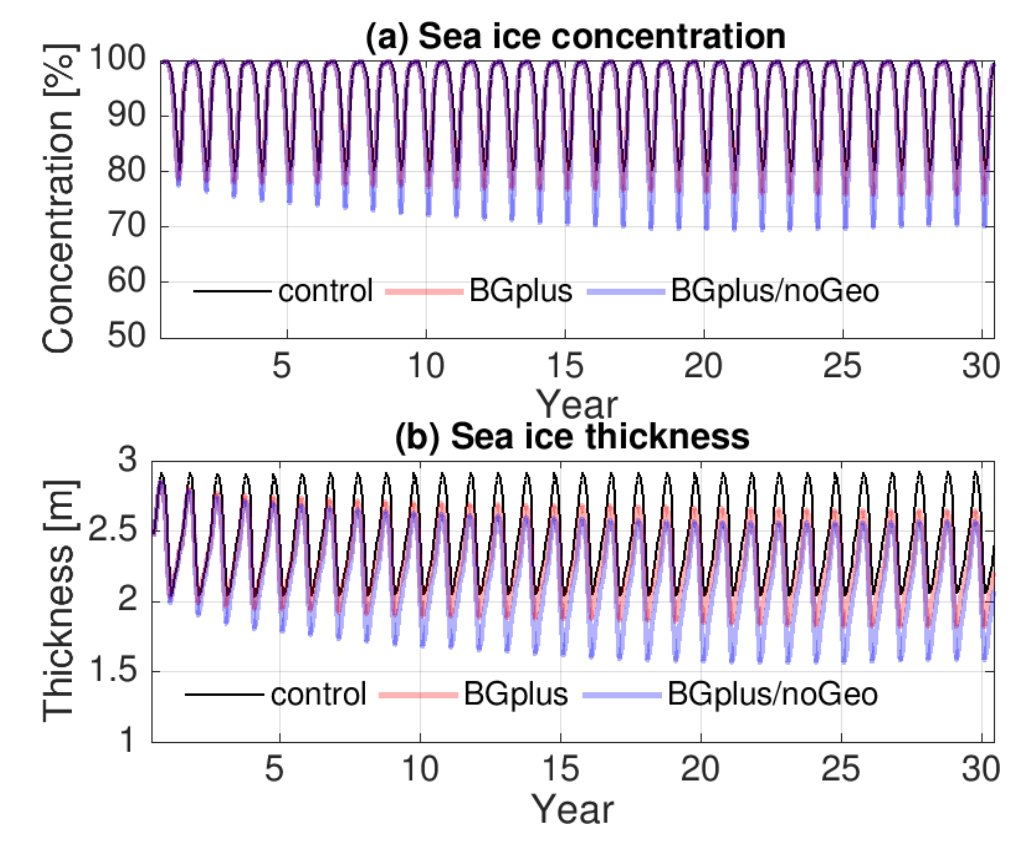
Supporting Information, Figure S2: (a) Time series of the liquid freshwater content (FWC) in the Beaufort Gyre (BG) region. (b) Time series of Ekman pumping in the BG region. Annual means are shown together with monthly means. The results are for the 'reference' experiment.



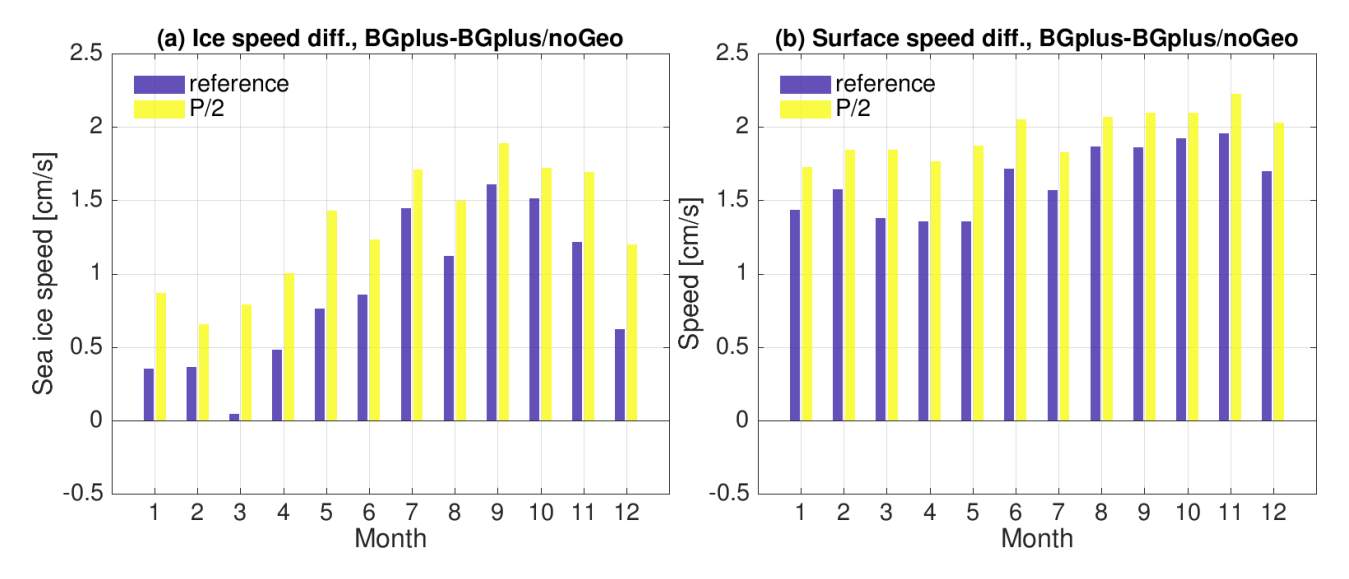
Supporting Information, Figure S3: The anomaly of the sea ice speed over the Beaufort Gyre (BG) refereced to the control run: (a) in the first year, (b) averaged from year 6 to year 15, (c) averaged from year 16 to 30. The results are for the 'reference' experiment.



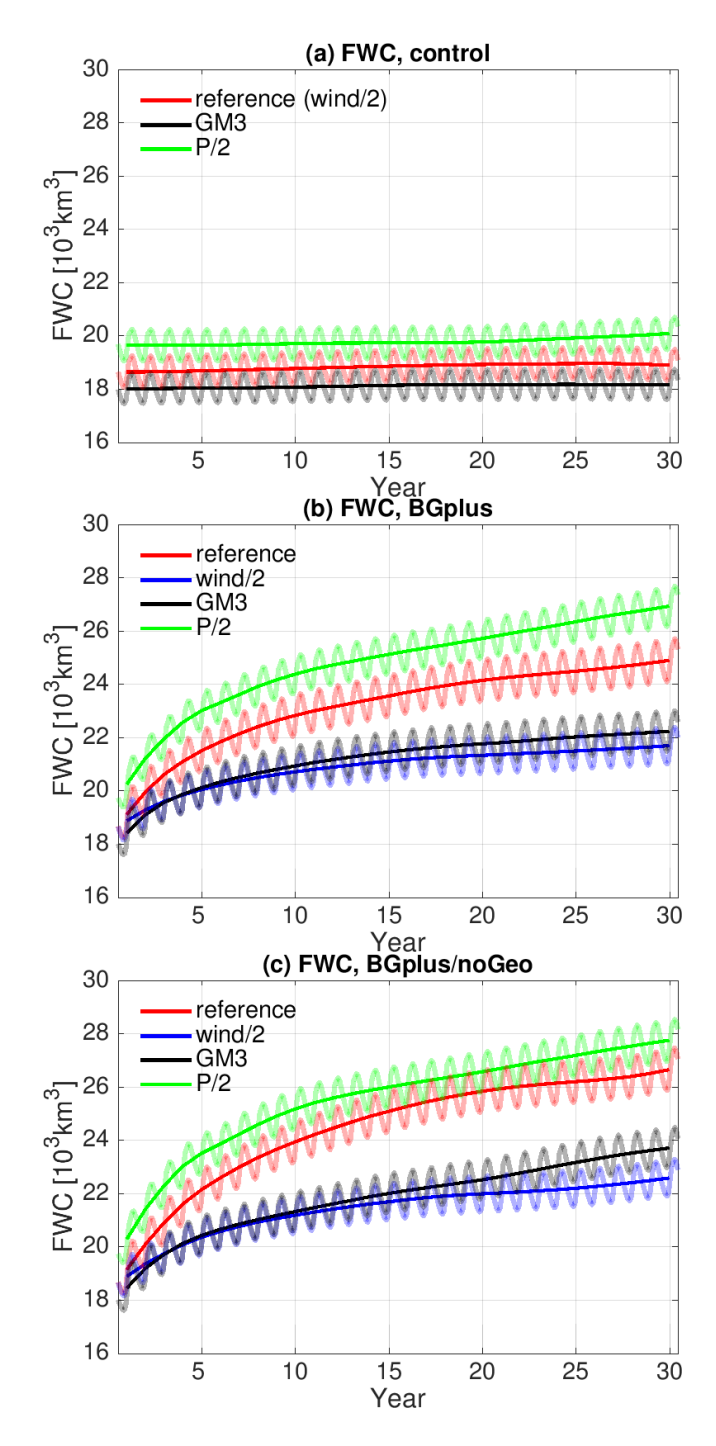
Supporting Information, Figure S4: The anomaly of the ocean surface speed over the Beaufort Gyre (BG) refereced to the control run: (a) in the first year, (b) averaged from year 6 to year 15, (c) averaged from year 16 to 30. Note that the speed in BGplus/noGeo is the modified one that is used in the calculation of ocean-ice stress. The results are for the 'reference' experiment.



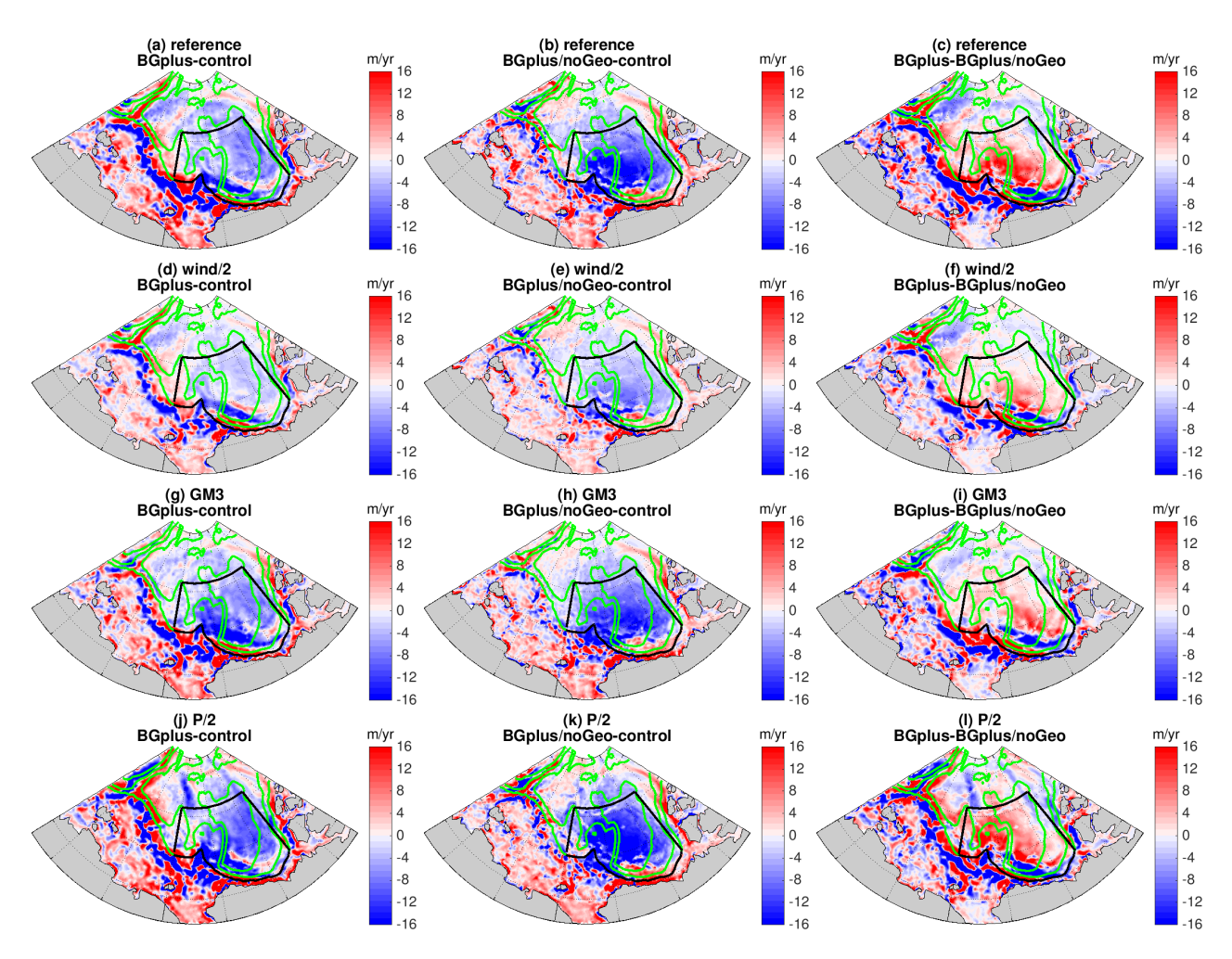
Supporting Information, Figure S5: The monthly time series of sea ice (a) concentration and (b) thickness in the Beaufort Gyre region in the reference experiment.



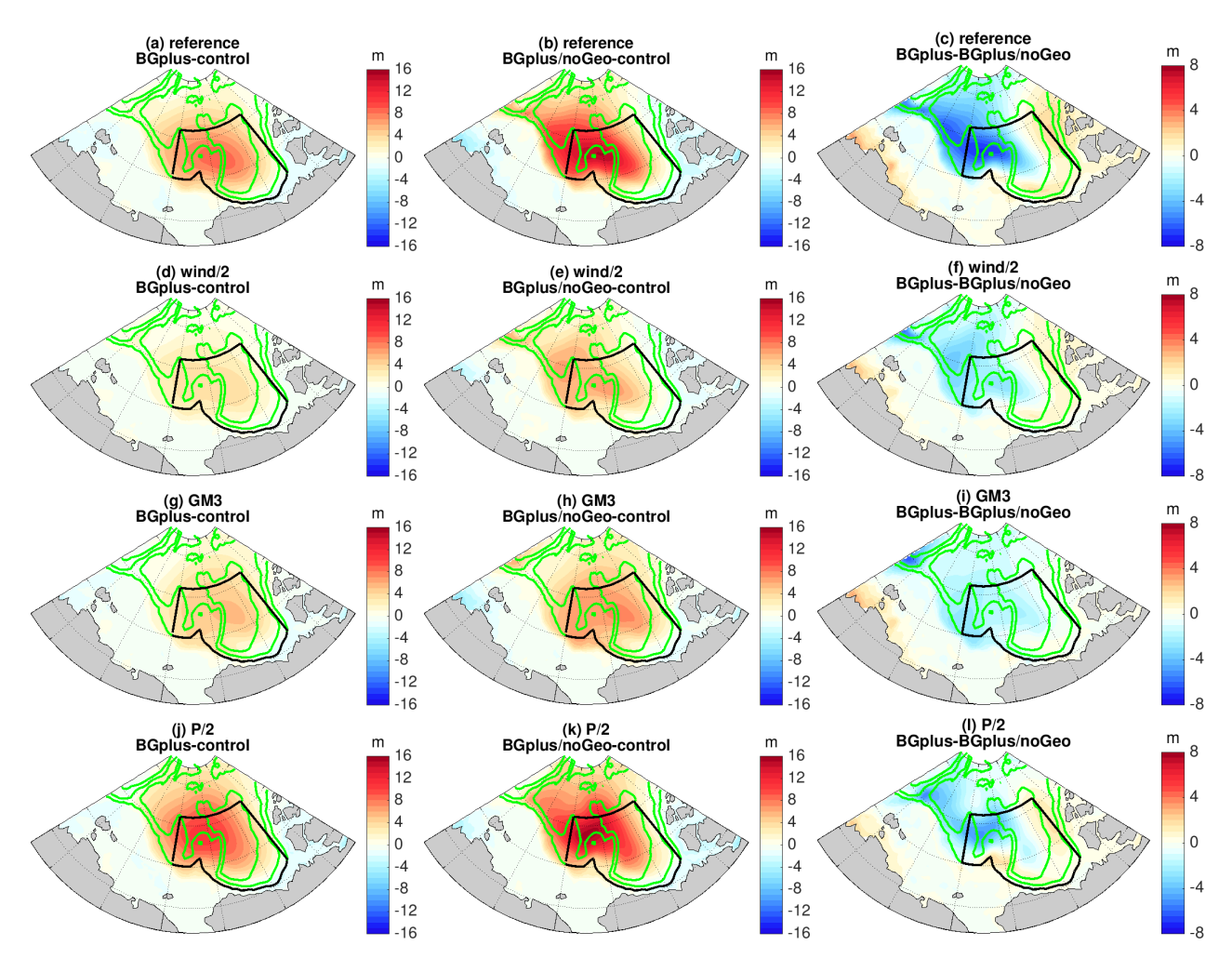
Supporting Information, Figure S6: (a) The difference of the Beaufort Gyre (BG) region sea ice speed between BGplus/noGeo and BGplus. (b) The same as (a) but for the ocean surface speed. In (b) the speed is the one used in the calculation of ice-ocean stress. Here we compare the P/2 experiment to the reference experiment.



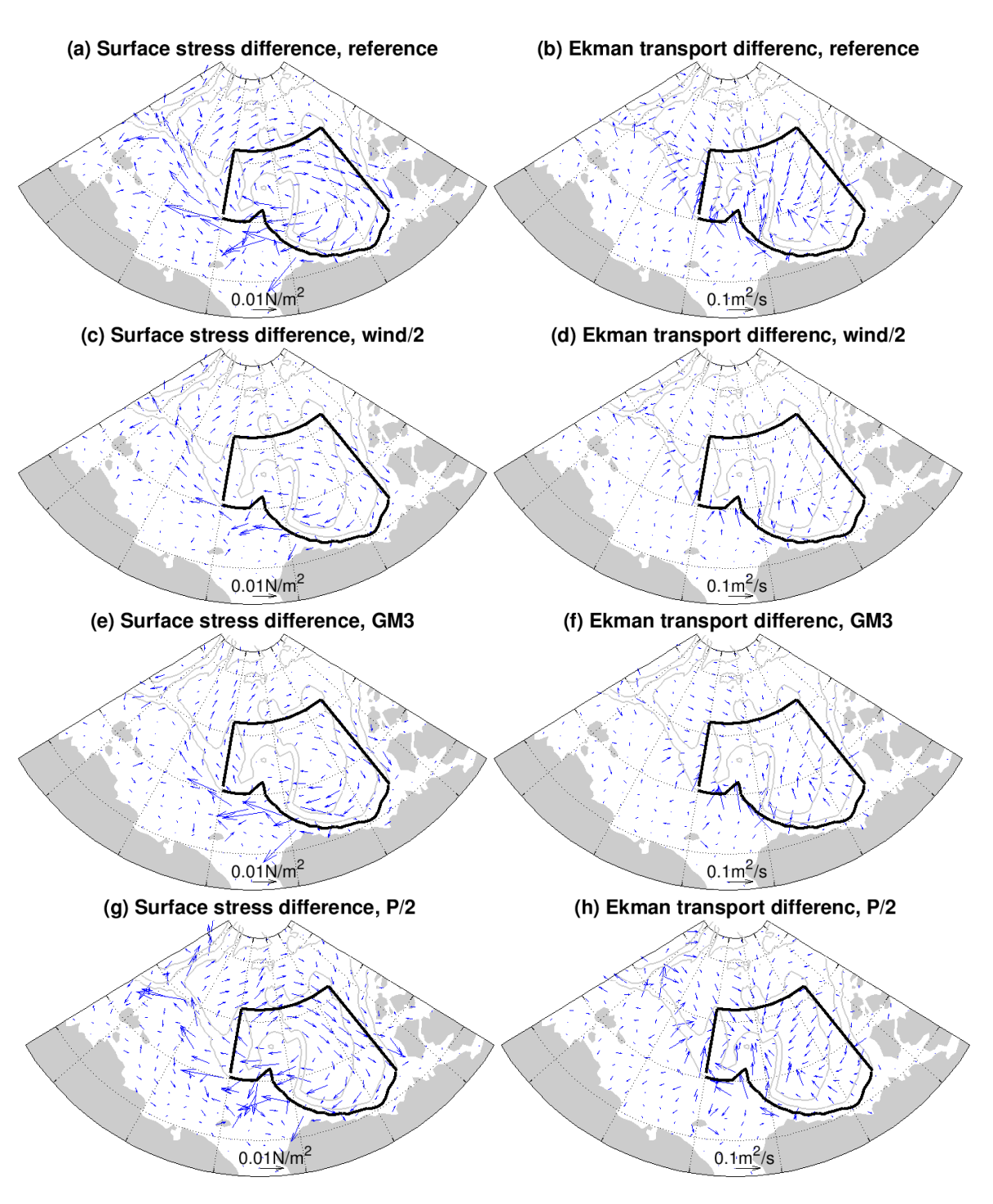
Supporting Information, Figure S7: Time series of Beaufort Gyre (BG) liquid freshwater content (FWC) in (a) control, (b) BGplus and (c) BGplus/noGeo in different experiments. The annual means are shown together with monthly means.



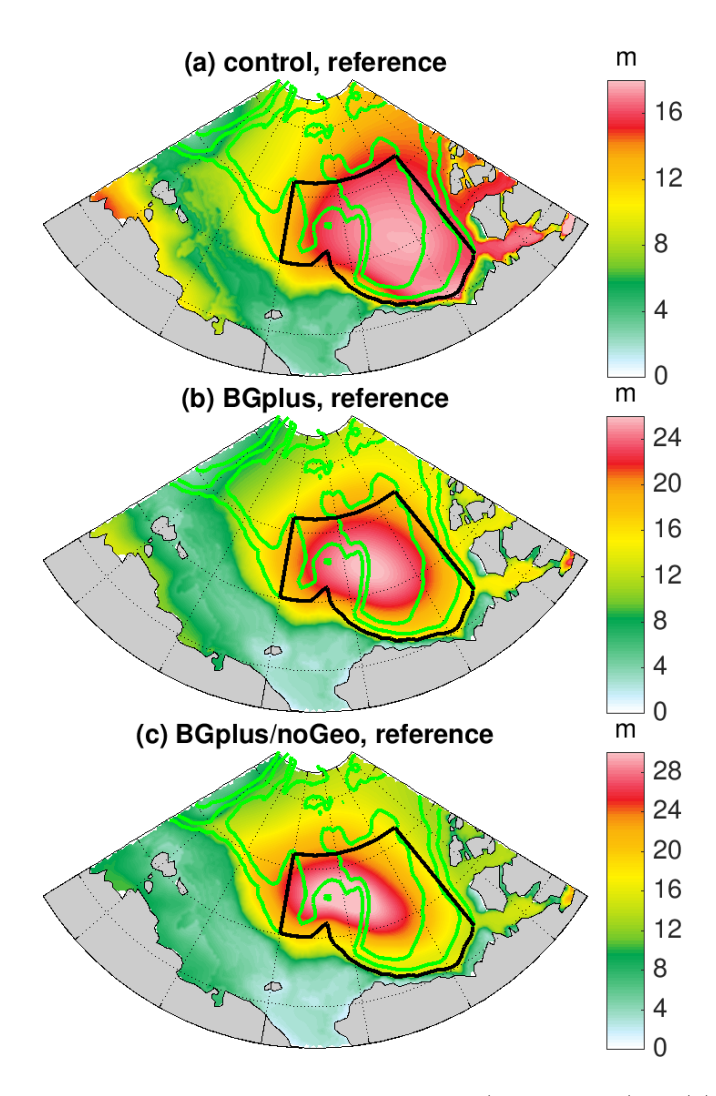
Supporting Information, Figure S8: The difference of the Ekman pumping between (a) BGplus and control, (b) BGplus/noGeo and control, (c) BGplus and BGplus/noGeo (the former minus latter) averaged over the last 5 model years for the 'reference' experiment. (d)(e)(f) The same as (a)(b)(c), but for the 'wind/2' experiment. (g)(h)(i) The same as (a)(b)(c), but for the 'GM3' experiment. (j)(k)(l) The same as (a)(b)(c), but for the 'P/2' experiment. The green contour lines indicate the 500 m, 2000 m and 3500 m isobaths. The black box indicates the Beaufort Gyre region.



Supporting Information, Figure S9: The difference of the liquid freshwater content (FWC, in m) between (a) BGplus and control, (b) BGplus/noGeo and control, (c) BGplus and BGplus/noGeo (the former minus latter) averaged over the last 5 model years for the 'reference' experiments. (d)(e)(f) The same as (a)(b)(c), but for the 'wind/2' experiment. (g)(h)(i) The same as (a)(b)(c), but for the 'GM3' experiment. (j)(k)(l) The same as (a)(b)(c), but for the 'P/2' experiment. Note that the color range in the rightmost column is different from that in the other two columns. The green contour lines indicate the 500 m, 2000 m and 3500 m isobaths. The black box indicates the Beaufort Gyre region.



Supporting Information, Figure S10: (a) The difference of the ocean surface stress between BGplus/noGeo and BGplus (the former minus latter). (b) The difference of the surface Ekman transport between BGplus/noGeo and BGplus (the former minus latter). The results are averaged over the last 5 model years for the 'reference' experiment. (c)(d) The same as (a)(b), but for the 'wind/2' experiment. (e)(f) The same as (a)(b), but for the 'GM3' experiment. (g)(h) The same as (a)(b), but for the 'P/2' experiment. The gray contour lines indicate the 500 m, 2000 m and 3500m isobaths. The black box indicates the Beaufort Gyre region.



Supporting Information, Figure S11: Liquid freshwater content (FWC, in m) in (a) control, (b) BGplus and (c) BGplus/noGeo simulations of the reference experiment. The purpose of this figure is to show the changes in the gyre center location, so color ranges are different between the figure panels to better visualize the gyre center. The green contour lines indicate the 500 m, 2000 m and 3500 m isobaths. The black box indicates the Beaufort Gyre region.